Technical report; TR-231

KNMI

The Conveyor Belt in the OCCAM model

tracing water masses by a Langrangian methodology

Trémeur Balbous and Sybren Drijfhout

Koninklijk Nederlands Meteorologisch Instituut

De Bilt, 2001

Technical Report = Technisch Rapport; TR-231

De Bilt, 2001

PO Box 201
3730 AE De Bilt
Wilhelminalaan 10
http://www.knmi.nl
Telephone +31 30 220 69 11
Telefax +31 30 221 04 07

Authors: Trémeur Balbous and Sybren Drijfhout

UDC: 551.465.5
551.46.062
167.7.001.573

ISSN: 0169-1708

ISBN: 90-369-2188-0

● ● ● ●

The Conveyor Belt in the OCCAM model

tracing water masses by a Lagrangian methodology

Master internship's report

September 18, 2000

Trémeur BALBOUS
Maîtrise of Applied Physics
University of Paris 6 (France)

Dr Sybren DRIJFHOUT
KNMI
De Bilt (Holland)

Contents

Acknowledgments

I would like to thank Dr Sybren Drijfhout who received me at KNMI and advised me all along this three months. I sincerely thank Dr Pedro De Vries for his help and the time he spared me. Thanks to Caroline for her bike, it was so handy, and John who gave me the chance to learn the last famous Anouk's song by listening it almost 15 times a day :). I also thank all the rest of the team for their welcome and their contentment.

Chapter 1

Introduction

On the global scale, the ocean circulation is driven by wind forcing and by fluxes of heat and fresh water through the surface. The circulation forced by the latter is called the thermohaline circulation. The part of the thermohaline circulation that is associated with the deep water formation in the North Atlantic Ocean and it compensating return flow is known as the Conveyor Belt. We can describe the Conveyor Belt by considering a water parcel flowing northward in the North Atlantic Ocean, becoming heavy by cooling and "sinking" into the deep ocean. This water parcel flows southward in a western boundary current to the South Atlantic Ocean where it reaches the Atlantic Circumpolar Current (ACC). From there it flows into the Indian and Pacific Ocean where it locally upwells. The particle finally flows back to the North Atlantic Ocean in the upper layers of the ocean through the South Atlantic and the Indian Oceans.

This work takes place in the TRACMASS project, which main goals are to establish the origin, the formation, the fate and the transformation for the North Atlantic Deep Water (NADW), to provide theoretical studies of the trajectory methods. To perform this, the TRACMASS team uses a new method that employs Lagrangian trajectories to investigate the North Atlantic water masses circulation obtained from numerical simulations of the global ocean. Three different models are used : two depth coordinate models and one density coordinate model.

In this context, the aim of our work, at KNMI, is to establish the transport and the routes of both NADW and it return flow simulated by the high resolution global ocean model "OCCAM". Routes are calculated from the Atlantic Equator to three sections : Drake Passage, Indonesian Throughflow, and South Australia, (supposed to be the origin of three different pathways of the NADW return flow to North Atlantic).

The results we obtained will be presented and discussed hereafter, but first of all, I will give an overview of the global ocean thermohaline circulation and a more detailed view of the Conveyor Belt. Thereafter I will explain the Lagrangian trajectory method, some details of the OCCAM model and of the

outputs we used.

Chapter 2

What is the Conveyor Belt?

The world ocean is an essential component of the physical climate system. This is related to the physical properties of sea water :

low Albedo when unfrozen, high Albedo when frozen (large influence on the atmospheric radiative balance);

large heat capacity (provide a long term memory for the climate system);

but also to the ocean dynamics :

the northward heat flux by the Conveyor Belt is comparable to the poleward one provided by the atmosphere;

at the ocean surface, there is a continuous exchange of heat and freshwater between ocean and atmosphere. These fluxes cause temperature and salinity gradients of sea water, which are responsible for density gradients which consequently drive a circulation commonly called thermohaline circulation.

So changing in the ocean thermohaline circulation can have some effects on the climate variability. And it is a reason of the increasing interest on improving our knowledge of the ocean thermohaline circulation.

The part of the thermohaline circulation that is associated with the southward flow of the deep-water mass that is formed in the North Atlantic Ocean (NAO) and it northward return flow is called the Conveyor Belt (Broecker, 1991). The Conveyor Belt scheme can be split in two compensating branches : the deeper one is outflow of the North Atlantic Deep Water (NADW) in the World Ocean, the shallow one consists of the return flow in the upper layers of the ocean.

The North Atlantic Deep Water

First consider a warm salty water parcel flowing northward at the surface of the NAO. As long as this parcel is in the surface mixed layer the atmospheric fluxes of heat and freshwater continuously alter its properties.

In the northern part of the NAO, during winter, the water particule is cooled by evaporation that is due to winter storms. This cooling and the stratification of the water increase the density and the water column becomes unstable.

The water column converts, and mixes vertically : the water particle "sinks" to the deep ocean. The deep convection, occurs in the NAO in the Greenland Sea and in the Labrador Sea (Killworth 1983). The downward transport is estimated to be inbetween 15 and 20 SV (1 Sv = $10^6 m^3/s$) (Gordon, 1986).

The NADW flows southward in a western boundary current to the South Antarctic Ocean (SAO), where it joins either the Antarctic Circumpolar Current (ACC) or the Indian Ocean south of Cape Agulhas. In the ACC NADW is converted into Circumpolar Deep Water (CDW) and it flows either northward into the Indian and Pacific Oceans or around the Antarctic.

Finally the water particle upwells, and it flows back into the NAO.

The NADW return flow

Historically, two routes are suggested for the NADW return flow : the "cold water route" and the "warm water route". In the "cold water route", the flow through the Drake Passage passes eastward into the SAO (Georgi, 1979; Piola and Georgi, 1982; McCartney, 1977). In the "warm water route", the Indian Ocean thermocline water flows westward into the SAO south of Africa and reach the NAO in the Bengulas Current (Gordon 1985).

Gordon (1986) argues that the CB is closed primarily by the "warm water" path. He argues that the thermocline water is returned to the North Atlantic by the following route:

1. The NADW introduced into the Pacific Ocean is transferred as North Pacific Central (thermocline) Water to the Indian Ocean through the Indonesian seas.

2. The Pacific water crosses the Indian Ocean in the 10^O-15^OS latitude belt, incorporating the saltier Indian Ocean thermocline water.

3. The mix of the Pacific Ocean and the Indian Ocean water passes southward within the Mozambique Channel, supplying a small component of the Agulhas Current transport.

4. A branch of the Agulhas Current flows into the South Atlantic and does not participate in the Agulhas retroflection, which returns most of the Agulhas water to the Indian Ocean.

5. The warm water passes northward with the South Atlantic subtropical gyre, crossing the equator to enter the upper layer of the North Atlantic.

The volume transport at the equator is inbetween 14 Sv and 17 Sv, estimated by numerical studies and measurements.

On the other hand, Rintoul (1991), calculating the heat transport by an inverse model suggested that the "cold water route" dominates completely the "warm water route" (Gordon,1986).

More recent results from numerical simulations seems to confirm that this route neither is insignificant nor dominant. These results also suggest that a part of the "cold water" route might be indirect : some of the water from Drake Passage may recirculate in the Indian Ocean subtropical gyre before reaching the NAO with the "warm water" route (Gordon et al., 1992, Döös, 1995).

Some of these studies seems to confirm a third route, that is a contribution source for the NADW return flow. Intermediate water coming from the Pacific Ocean, flowing south of Australia reaches the north of Madagascar in the subtropical gyre current and flows in the Mozambique Channel (Speich et al. 2000). Then it spreads to NAO in the "warm water" route. This westward flow has been documented before that by Reid (1986), Fine (1993), Döös (1995). Results from Rintoul and Bullister (1999) and Ganachaud's (1999) inverse models confirmed the presence of such a flow of Intermediate Water between the sea surface and the layer extending down to 1200m.

It is easy to understand that the South Atlantic Ocean, connected to both the Indian and Pacific Oceans, is a crucial region for the Conveyor Belt. It receives NADW from the NAO, it distributes this among the Global Ocean and it gives back to the NAO the similar volume of lighter water. The Conveyor Belt scheme has been developed during the last fifteen years, and lots of questions still remain, for instance, about the location of upwellings, the volume of water masses transported, their origins and routes.

So, in the following study, we will try to figure out evidences of these routes in the high resolution global ocean OCCAM model. We will also estimate values of the water mass transport, by calculating the volume transport for the NADW : from the Atlantic Equator to Drake Passage, Indonesia through flow, and South Australia. But also it return flow : from the Drake Passage, Indonesia through flow, and South Australia to the Atlantic Equator.

Chapter 3

Methodology

3.1 The OCCAM model

The OCCAM project has developed two high resolution (1/4 and 1/8 degree) models of the World Ocean - including the Arctic Ocean and marginal seas such as the Mediterranean. The project is being carried out by researchers at the Southampton Oceanography Centre in collaboration with colleagues from the Universities of East Anglia and Edinburgh.

The model is run on the UK Research Councils' multi- processor Cray-T3D operated by the University of Edinburgh. The initial model run for 12 model years has been completed on September 1996. The results are used to understand the heat flows and movements of different water types in the ocean. They are also used to help analyse the data from WOCE, the World Ocean Circulation Experiment.

TRACMASS simulation

The TRACMASS simulation uses a 0.25 degree resolution both in latitude and longitude. The model covers the full globe from 78.5°S to 90°N. The vertical resolution varies, from 10m near surface, to 250m at 5500m with a total of 36 levels. It uses a 5'x5' ETOPO5 topography .

OCCAM is a primitive equation numerical model of the global ocean. It is based on the GFDL MOM version of the Bryan- Cox- Semtner ocean model but includes a free surface and improved advection schemes.

It uses a normal Laplacian diffusion and momentum terms to represent horizontal mixing. For diffusion of tracers the value of the horizontal diffusion coefficient is $1*10^6 cm^2/s$. For the velocity field the horizontal viscosity is $2*10^6 cm^2/s$. After day 480 the model uses Pacanowski and Philander (1981) vertical mixing for the tracer fields. The velocity fields use normal Laplacian mixing in the vertical with a coefficient of $1 cm^2/s$. A regular longitude-latitude grid is used for the Pacific, Indian and South Atlantic Oceans. A rotated longitude-latitude grid is used for the Arctic and North Atlantic Oceans, which has its poles on the

equator in the Indian and Pacific Oceans. This overcomes the singularity that otherwise arises at the North Pole. A simple channel model is used to connect the two grids through the Bering Strait. The model also uses a finite differences discretisation based on a staggered B-grid [Arakawa, 1972]. The model depths are based on the ETOPO5 data set, with sill depths checked against original surveys.

The model was started from the Levitus annual mean temperature and salinity fields. The surface forcing uses a set of mean monthly winds derived from ECMWF wind stressed for 1986-88 and a surface relaxation to monthly Levitus [1994] SST (30 days timescale). The fresh water is derived from the salinity differences between the model and monthly Levitus [1994] surface salinities. The difference is converted to a freshwater flux which drives a volume change via the sea surface height field.

The first 12 model years run has been continued during 3 years using a high frequency wind surface forcing : 6-hourly ECMWF wind-stresses (1993, 1994, 1995). The TRACMASS data set is based on the last three years and contains : sea level, potential temperature, salinity and velocity with a 5-days resolution in time (219 files).

3.2 The Lagrangian methodology

Ocean models have historically described the ocean circulation in terms of Eulerian quantities. They provided velocity, salinity fields and others characteristics at discrete points in the ocean, as functions of time. That is what most ocean instruments measure.

Nowadays new methods of instrumentation involve Lagrangian measurements by instruments drifting with the flow. Also, a new technique to analyse data and derive further information is to consider Lagrangian trajectories (Döös, 1995; Blanke and Raynaud, 1997).

Blanke and Raynaud (1997) showed that the trajectory inside one grid box can be given analytically assuming a linear interpolation of the velocities. An entire trajectory then consists of subsequent calculations of positions on the edges of grid boxes. Forward and backward integrations are both possible. In this way, very large quantities of trajectories can be generated accurately and efficiently providing a powerful tool to carry out off-line investigations of large data sets. In addition, by assigning certain mass transports to particular trajectories (Döös, 1995; Blanke and Raynaud, 1997), quantitative measurements of water mass exchanges between different ocean basins or sections can be obtained. For a proper analysis one generally needs tens of thousands trajectories. Within this approach a specific water mass is represented by a large ensemble of smaller water parcels, each representing in a averaged sense a collection of water molecules. Temperature and salinity budgets along trajectories can be computed in order to assess water mass transformations (Drijfhout et al., 1996). Convection can

be taken into account by assigning a water parcel a random depth whenever it enters a convectively unstable water column (Döös, 1995; Drijfhout et al., 1996). Like the velocities used to calculate the trajectories, these convection events also follow from the ocean model.

In our study, we will use Lagrangian trajectories calculated using the three dimensional stationary velocity fields from the OCCAM data sets. We will trace forward the NADW masses and backward it return flow masses from the Atlantic Equator to three different sections : Drake Passage, Indonesian Throughflow, South Australia. And we will represent then the Lagrangian streamfunctions : the zonal integration, at each time-step, of the volume transports that is associated to each trajectory. The transport associated to a water mass at a section is the integration of the streamfunctions associated to trajectories ended at the considered section for the considered water mass.

From velocities considered to be known on the corners of the "B" grid boxes of OCCAM, volume transport is derived. The volume transport through the eastern wall of the ijk grid box is given by

$$U_{i,j,k} = \frac{1}{2}(u_{i,j,k} + u_{i,j-1,k})\Delta y \Delta z_k, \tag{3.1}$$

in which i, j, k denote the discretised longitude, latitude and depth, respectively, u are zonal velocities and $\Delta y \Delta z$ defines the meridional-vertical area. Meridional transports are defined analogously, while vertical transports simply follow from the non divergency of the velocities.

Inside a grid box, Figure (3.1), volume transports are obtained by interpolating linearly between the values of the opposite walls. For the zonal direction, using $F_i = U_{i,j,k}$ and $r = x/\Delta x_j$ one obtains

$$F(r) = F_{i-1} + (r - r_{i-1})(F_i - F_{i-1}). \tag{3.2}$$

Local transport and position are related by $F = dr/ds$, where the scaled time variable $s = t/(\Delta x_j \Delta y \Delta z_k)$ [the dominator being the volume of the particular grid box]. Equation (3.2) can now be written in terms of the following differential equation

$$\frac{dr}{ds} + \beta r + \delta = 0, \tag{3.3}$$

with $\beta = F_{i-1} - F_i$ and $\delta = -F_{i-1} - \beta r_{i-1}$. Using the initial condition $r(s_0) = r_0$, the zonal displacement of the trajectory inside the considered grid box can be solved analytically and is given by

$$r(s) = (r_0 + \frac{\delta}{\beta}) \exp_{-\beta(s-s_0)-\frac{\delta}{\beta}}. \tag{3.4}$$

The time s_1 when the trajectory reaches a zonal wall can be determined explicitly

$$s_1 = s_0 - \frac{1}{\beta} \log \left[\frac{r_1 + \delta/\beta}{r_0 + \delta/\beta} \right], \tag{3.5}$$

where $r_1 = r(s_1)$ is given by either r_{i-1} or r_i. With the use of (3.2), the logarithmic factor can be expressed as $\log[F(r_1)/F(r_0)]$. For a trajectory reaching the wall $r = r_i$, for instance, the transport $F(r_1)$ must necessarily be positive, so in order for Equation (3.2) to have a solution, the transport $F(r_0)$ must then be positive also. If this is not the case, then the trajectory either reaches the other wall at r_{i-1} or the sign of the transports are such that there is a zero zonal transport somewhere inside the grid box that is reached exponentially slow.

For the meridional and vertical directions a similar calculation of s_1 is performed determining, respectively, the meridional and vertical displacements of the trajectory inside the considered grid box. The smallest transit time $s_1 - s_0$ and the corresponding r_1 denote at which wall of the grid box the trajectory will exit and move into the adjacent one. The exact displacements in the other two directions are the computed using the smallest s_1 in the corresponding expressions (3.4). the entire procedure is then repeated for as long is desired.

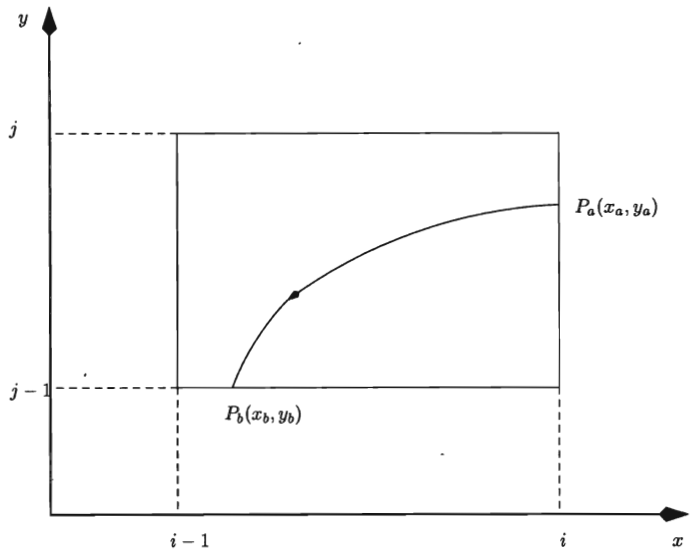

Figure 3.1: Illustration of the trajectory path through one grid box, where the model velocities are at the four corners of the box

3.3 Investigation parameters

3.3.1 Data files

We used three different data sets, so three different stationary (annual averaged) velocity fields : one original and two "reanalysed", to calculate the trajectories and plot the corresponding streamfunctions. That will allow us to compare the occuracy of original data set from the OCCAM model, and the "reanalysed"

velocity fields in resolving the Conveyor Belt routes associated to different water masses. The water masses are defined by their potential density σ. For the upper branch of the Conveyor Belt or the NADW return flow we used σ_0 defined as $\sigma_0 = (\rho(s,t,0) - 1000)kgm_{-3}$ and for the deeper branch : NADW, we used σ_2 that is defined at 2000m depth.

ann.mean1 : time averaging at fixed depth z

This is the "original" data set from OCCAM. It contains 5 day-runnings averaged outputs, averaged then overtime to annual mean velocity, salinity temperature and density fields.

bolus1.dat : time averaging at constant potential density σ

Mass transport of a certain water mass, defined to lie within a certain density range is most easily calculated at density surfaces, that is, with density as a vertical coordinate instead of depth. Mass transport is gouverned by the following equation :

$$\frac{\partial h}{\partial t} + \nabla.\vec{u}h = \Delta W_{dia},$$

where h is the density-layer thickness, $\vec{u} = (u, v)$ is the horizontal velocity and ΔW_{dia} is the net diapycnic velocity across the density layer. The 3 year-averaged fields give:

$$\overline{\frac{\partial h}{\partial t}} + \nabla.\overline{\vec{u}h} + \nabla.\overline{\vec{u}'h'} = \Delta\overline{W}$$

The overline denotes the time average, $\vec{u} = \overline{\vec{u}} + \vec{u}'$, $h = \overline{h} + h'$ and $\overline{\vec{u}'h'}$ is called bolus transport.

In steady state : $\overline{\frac{\partial h}{\partial t}} = 0$ and the layer integrated average of $\overline{W}$ is $\left[\Delta\overline{W}\right] = 0$.

In an eddy-permitting model, $\overline{\vec{u}'h'}$ can be nonzero. This term is therefore important to onclide when describing the transport of water masses. The importance of bolus velocity in advecting water mass has been demonstrated in ocean global circulation models (Danabasoglu et al., 1994; Gent et al., 1995) where the bolus velocity is parametrised and in idealised eddy resolving model (Lee et al., 1997) where the bolus velocity is diagnosed.

The importance of bolus velocity in eddy-permitting model such OCCAM model has not been explicitely calculated. So, in order to estimate the eddy-induced mass transport, we are using a velocity field that is the exact bolus velocity. We now have an expression of volume transport $\widehat{V} = \overline{V} + U^*$ where $\overline{V}$ is the averaged volume transport and U^* is the bolus transport contribution.

btrennew.dat : correction for the model drift

When the model drifts, a correction is necessary. We remove the drift by writing:

$$\nabla\left(\overline{\vec{u}h} + \overline{\vec{u}'h'}\right) + \nabla\vec{U_c} = \overline{\Delta W_c},$$

where $\overline{\Delta W_c} = 0$ and the "flux" $\vec{U_c}$ is calculated using the equation

$$\nabla.\vec{U_c} = \overline{\frac{\partial h}{\partial t}} - \overline{\left[\frac{\partial h}{\partial t}\right]}$$

.

So we now have the transport : $V_{new} = \widehat{V} + U_c$ where U_c is the drift transport contribution.

spring1.dat, summer1.dat, autumn1.dat, winter1.dat : time averaging at constant potential density σ for each season

The seasonal datafiles have been produced using the exact bolus velocity calculation. Instead of using all data, we used seasonal data.

3.3.2 Density classes

Some previous Lagrangian trajectories computations from OCCAM velocity fields fixed the turning point between NADW and it compensating flow in the upper branch of the Conveyor Belt at the critical density $\rho_{crit} = 1027.625 kg/m_3$. We will trace water masses, from the equator forward in time for NADW and backward in time for the surface water, to Drake Passage (70^{O}W), Indonesian Throughflow (120^{O}W) and South Austrlia (147^{O}E). But we first have to define the density classes.

Deep layer waters

At the Atlantic Equator the water masses with a σ_2 potential density above 36,8 and flowing southward are considered to be NADW. These total water mass is divided in three classes as follow :

Upper North Atlantic Deep Water (UNADW) ($36.6 < \sigma_2 \leq 37.0$)

Middle NADW (MNADW) ($37.0 < \sigma_2 \leq 37.1$)

Low NADW (LNADW) ($\sigma_2 > 37.1$)

Upper layer waters

At the Atlantic Equator, σ_0 potential density smaller than 27.6 and northward flow, is used to defined the NADW return flow, which is composed of SACW, SAMW, AAIW, UCPW as defined hereafter :

the South Atlantic Central Water (SACW) ($\sigma_0 \leq 26.5$);

the South Atlantic Mode Water (SAMW) ($26.5 < \sigma_0 \leq 27.0$);

the AntArctic Intermedate Water (AAIW) ($27.,0 < \sigma_0 \leq 27.4$);

the Upper CircumPolar Water (UCPW) ($27.4 < \sigma_0 \leq 27.6$);

the rest is the water particules which doesn't belong to the three density classes at the end of the trajectory.

Chapter 4

Results and Discussion

Water particle trajectories and associated transports have been calculated for both the upper and lower branch of the Conveyor Belt from OCCAM model annual mean data sets. That has been done between the Atlantic Equator and three sections as already mentioned, Drake Passage (70°W), Indonesian Throughflow (120°E), South Australia (147°E). And for different water masses defined at the Equator : UNADW, MNADW, LNADW for the NADW route and SACW, SAMW, AAIW, UCPW for it return flow. As mentioned earlier, for a proper analysis, one generally needs tens of thousands trajectories. So, to be consistent with that but also to manage an acceptable computing time, we decided to use a volume transport of 0.001 Sv per trajectory at the equator (which represents about 61000 trajectories calculated for annual data sets and about 75000 trajectories when using seasonal data sets). So that all the results below have been computed with that volume transport. The differences between results obtained calculations using trajectories representing 0.01 Sv and those representing 0.001Sv was about $\pm 0.15 Sv$ while they was only $\pm 0.05 Sv$ between initial elementary volume transports of 0.001 Sv and 0.0001 Sv.

In the following table and plot captions, the correspondence with the data files are :

annual mean : run with ann.mean1;

annual mean + contribution from exact bolus calculation : run with bolus1.dat;

annual mean + contribution from exact bolus calculation + contribution from detrending : run with btrennew.dat.

4.1 The upper branch of the Conveyor Belt : the NADW return flow

The results for the upper branch of the Conveyor Belt have been calculated with an initial volume transport of 0,001 Sv, for water masses that belong to SACW, SAMW, AAIW, UCPW at the Atlantic Equator and back-tracking them to Drake Passage (DRAKE), South of Australia (SAUS) and Indonesian Throughflow (ITFL) sections. The recirculation is the part of the water that flows back to the equator and enter the NAO (Recirc).

Quantitative results using annual data sets are presented in Tables (4.2, 4.3, 4.4). They emphasize some important differences, both for total transport values and partition in density classes of this total transport through the sections. For instance, even if the total volume transport through DRAKE is for the three data files, weaker than the sum of this total transport through ITFL and SAUS, it is relatively more important when we used the contribution from drift correction (at least +1.5 Sv). On the other hand, the flow from SAUS, which also appears in OCCAM model when using detrending calculation, is at least 1 Sv weaker. It represents only 3.1 Sv (compare to 4.2 or 4.6 Sv). But this number is comparable to the results suggested by the OPA model (Speich et al., 2000).

Moreover, our results are fully comparable to results from other calculations from both numerical studies and observations. We calculated a water mass transport of about 15 Sv at the equator (table 4.1 : D+I+S) which is a commonly accepted number for volume transport in the upper branch of the Conveyor Belt. This table, we can also say that most of the water at the Atlantic Equator is a upper thermocline water. The volume transport of SACW represents the same amount as transport of the three other water classes together. In this way, the circulation of SACW in the upper branch can be influenced by a modification of the atmospheric wind circulation. The vertical partition in density classes is different for the SAUS route. The water coming from DRAKE and ITFL is mainly SACW and SAMW, but the water from SAUS is figured out in all the density classes with more or less the same amount (about 1 Sv).

These general quantitative results are well represented when ploting the associated streamfunctions. We can denote on Figures (4.1, 4.2, 4.3) that are plotted from the detrended data set, for water masses defined at the equator and respectively backward traced to Drake Passage, Indonesian Throughflow and South Australia that both paths and strength of flows are really different from a section to an other. Water coming through Drake Passage into SAO, flows northward east of Falkland Island. At 45°S the flow turns right and joins the South Atlantic subtropical gyre. A part of the water mass recirculates in this gyre. It crosses the SAO by the Bengulas Current (BC) and it reaches the northward west boundary current between 30°S and 20°S. The water mass

Table 4.1: The volume transport has been calculated from btrennew1.dat at equator for water masses from each section. Results are in Sverdrups (1 Sv = 10^6 m^3s^{-1}).

Total	DRAKE	ITFL	SAUS	$D+I+S$
SACW	2.85	3.41	1.31	7.57
SAMW	1.23	1.88	0.74	3.84
AAIW	1.51	0.82	1.00	3.32
UCPW	0.19	0.06	0.09	0.35
Total	5.78	6.17	3.14	15.08

spreads into the NAO by this current. Another of this water mass enters the Indian Ocean and recirculates into the Indian Ocean subtropical gyre. Some of the water flows north of Madagascar and enters the Agulhas Current (AC) by Mozambique Channel (MC). A part of this water flows in the BC by the branch of the AC that does not participates in the Agulhas retroflection and reaches the equator by the same route as the direct "cold water" route. Water coming from ITFL flows directly through the Indian Ocean. Some of this water participates in the strong recirculation but most of it flows southward in the MC, then some reaches the BC and flows through the SAO to the boundary current. The water from ITFL reaches this boundary current between 28°S and 12°S. The other part of the water mass participates in the Agulhas retroflection. It could be interesting to note that the subtropical recirculation is weaker than the recirculation of water from DRAKE. Water from SAUS flows on a direct way through the Indian Ocean, enters the MC north of Madagascar and reaches the AC. This water does not participate in the retroflection but flows in the BC and reaches the boundary current between 28°S and 10°S.

These results are slightly different from a data file to an other. At DRAKE, for instance, the differences between the plot from ann.mean1 (fig 4.4) on one side and the plots from bolus1.dat and btrennew.dat (fig 4.5, 4.1) on the other side are important, while the difference between the latter are mainly on the strength. That denotes the importance of the bolus transport to modify both pathways and strength of water mass by advection. In Tables 4.3 and 4.4 the flow through DRAKE is stronger when we applied the detrending than using only the bolus calculation. But the pattern, that means the path of the water, is almost the same. Strength differences appear in the subtropical gyres in both the South Atlantic and the Indian Oceans, but not in the cross Atlantic BC. However, the flow in BC from detrended data set reach the boundary current more north. The Agulhas retroflection is also stronger when using the detrending, that could be explained by the fact that the detrending only occurs on the

The volume transports below have been calculated at each section for Tables (4.2, 4.3, 4.4) for water going to equator. For Table (4.1) at equator for water masses from each section. Results are in Sverdrups (1 Sv = 10^6 m^3s^{-1}).

Table 4.2: Transport calculated from annual mean.

Total	DRAKE	ITFL	SAUS	$D+I+S$	Recirc
SACW	0.03	4.69	0.02	4.74	20.59
SAMW	0.22	0.61	0.52	1.36	3.32
AAIW	0.74	0.62	1.79	3.15	1.54
UCPW	1.34	0.28	1.06	2.68	0.82
REST	1.43	0.07	0.78	2.28	22.02
Total	3.76	6.27	4.17	14.21	48.29

Table 4.3: Transport calculated from annual mean + contribution from exact bolus.

Total	DRAKE	ITFL	SAUS	$D+I+S$	Recirc
SACW	0.25	5.48	0.10	5.83	19.72
SAMW	1.95	0.66	2.46	5.07	3.44
AAIW	2.01	0.58	1.52	4.12	1.50
UCPW	0.01	0.34	0.41	0.77	0.76
REST	0.14	0.05	0.10	0.30	16.36
Total	4.36	7.12	4.60	16.09	41.79

Table 4.4: Transport calculated from annual mean + contribution from exact bolus calculation + contribution from detrending.

Total	DRAKE	ITFL	SAUS	$D+I+S$	Recirc
SACW	0.36	5.02	0.02	5.40	20.00
SAMW	1.99	0.55	2.03	4.57	3.86
AAIW	2.75	0.36	0.84	3.95	1.49
UCPW	0.14	0.21	0.15	0.51	0.74
REST	0.54	0.03	0.10	0.66	18.88
Total	5.78	6.17	3.14	15.09	44.97

divergence. On the other hand, the structure of the circulation when using the annual mean data file is really different and sometimes more complicated. The extension of the circulation is comparable (the water flows in the same regions) but the circulation cells are more diffused. The water mass volume transport is also weaker in these gyres. The structure of the flow, in the Agulhas retroflection area, where lots of eddies occur, is slightly more complicated. We also have a strong recirculation south of the circumpolar current that does not appear when using bolus calculation.

The water mass transport partition on the vertical scale through SAUS is interesting. Compare to the water mass partition through DRAKE and ITFL, the water masses are almost equally distributed in the first three layers of the flow. Moreover the route from SAUS is recently drawn to attention and not so much documented. The SAUS route (fig 4.3) is more or less direct from Tasmania to the Atlantic Equator. The water masses flow south of Australia, and reach the Indian Ocean subtropical gyre. There most of the water flow north of Madagascar in the MC, before entering the Agulhas current and the Bengulas current to the Atlantic Ocean. As mentioned, water masses flowing through SAUS are homogeneously shared in three water classes : SACW, SAMW and AAIW, the volume transport in fourth one : UCPW is negligible. But their pathways, near Madagascar are different. The upper layer waters : SACW and SAMW (fig 4.7 4.8), flow to north of Madagascar and enter in the MC while AAIW takes a south of Madagascar route.

Uptillnow, we only used, annually averaged data. We will now investigate the seasonal sensitivity of the water masses in the OCCAM model Conveyor Belt. In that aim, we analysed streamfunctions calculated from a unique season data set, that means only one season of the seasonally averaged data sets was used instead of an annually averaged data set. The results for waters flowing through ITFL, performed with perpetual winter (fig 4.10) and perpetual summer (fig 4.11 are the most different, but differences also occur for both other origins (DARKE and SAUS) and seasons. The vertical structure of the mass transports is also really different through the Indian Ocean, but it is not so much for the Atlantic Ocean route. With the perpetual winter data set, we observed a direct pathway from ITFL to Madagascar with two eastward extended recirculation, but a weaker Somalian Current. We also observed a strong Agulhas retroflection, whereas, with the summer data file, this retroflection is weakened, but the part of the water flowing through the SAO is increased. But there is much more activity at the Indian Equator with this last data set. The ITFL to Madagascar flow is also stronger for perpetual summer, but that difference is not evident in the MC, so maybe a large part of this westward flow recirculates in the North Indian Ocean.

The vertical structure of the transport for both perpetual winter and summer

are different. Using summer data set, the deeper water mass transport around the Indian Equator is really small compare to winter, whereas in the three other classes the transport is really stronger in that area. Around Cape Agulhas, the circulation seems to be mainly driven by the surface water when using summer data set whereas the deeper transport remain not negligible for AAIW and UCPW.

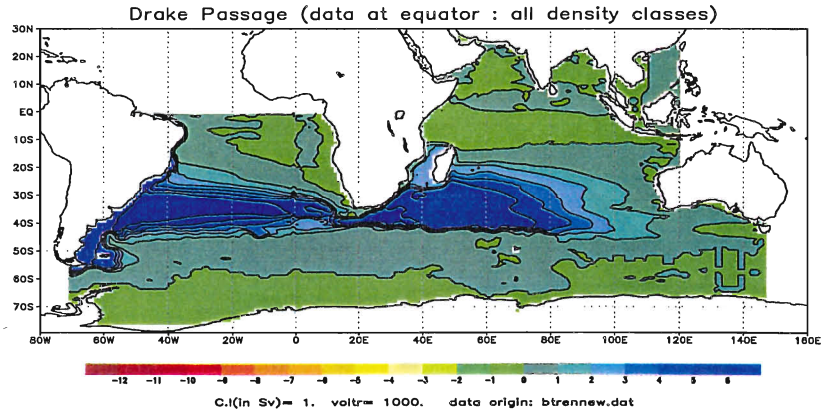

Figure 4.1: Drake section btrend data file

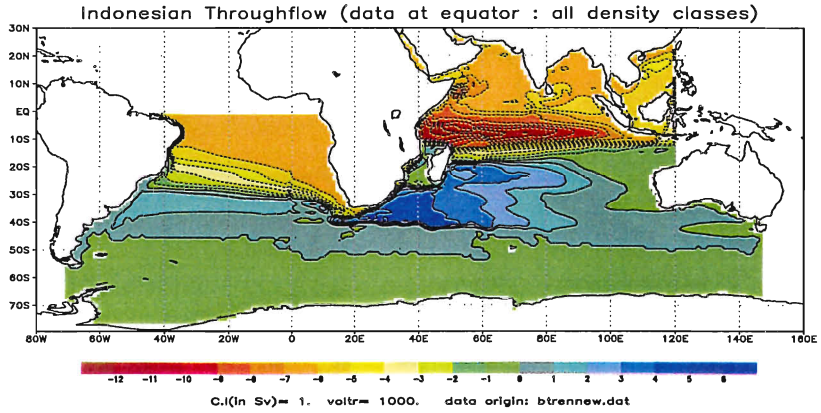

Figure 4.2: ITFL btrend data file

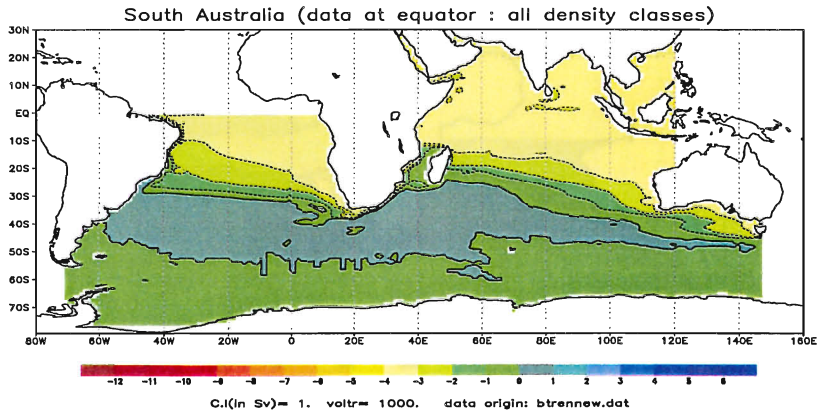

Figure 4.3: SAUS btrend data file

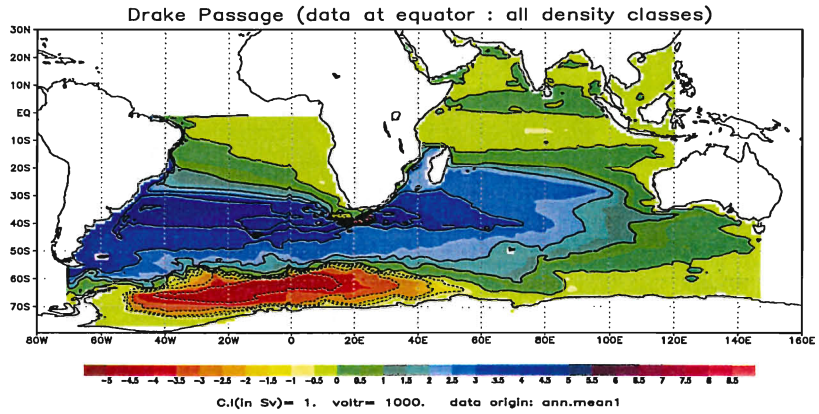

Figure 4.4: Drake section annual mean data file

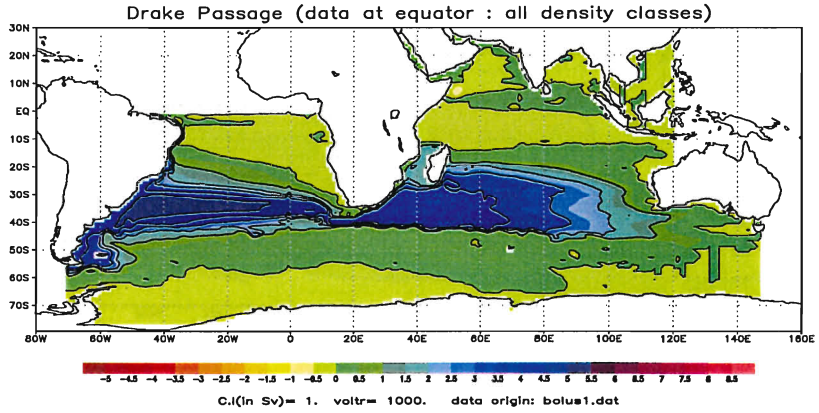

Figure 4.5: Drake section bolus data file

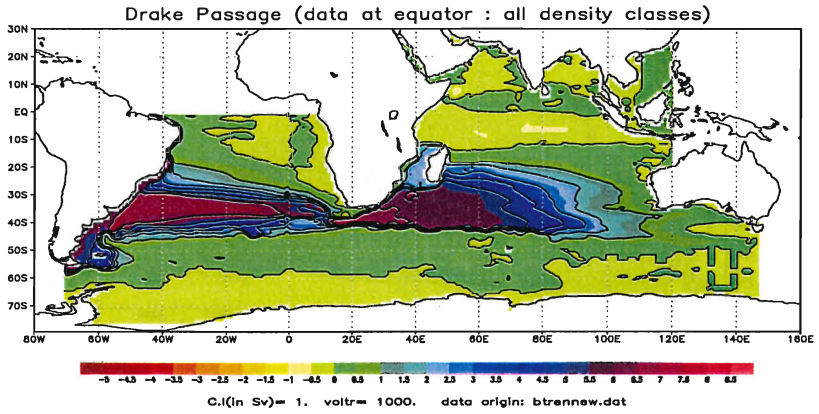

Figure 4.6: Drake section btrend data file

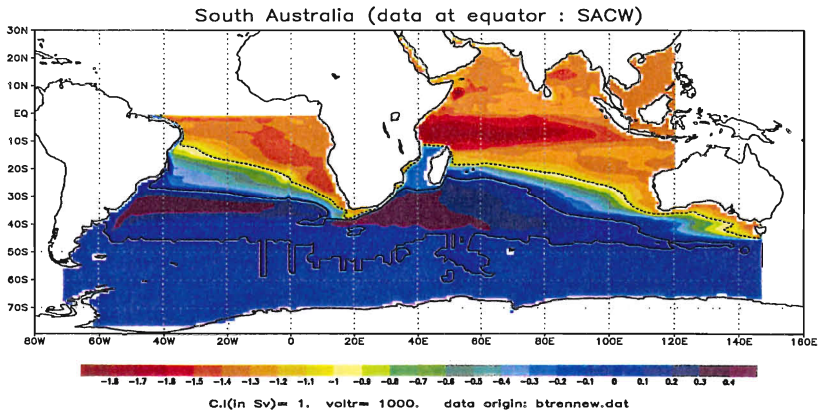

Figure 4.7: South Australia section btrend data file

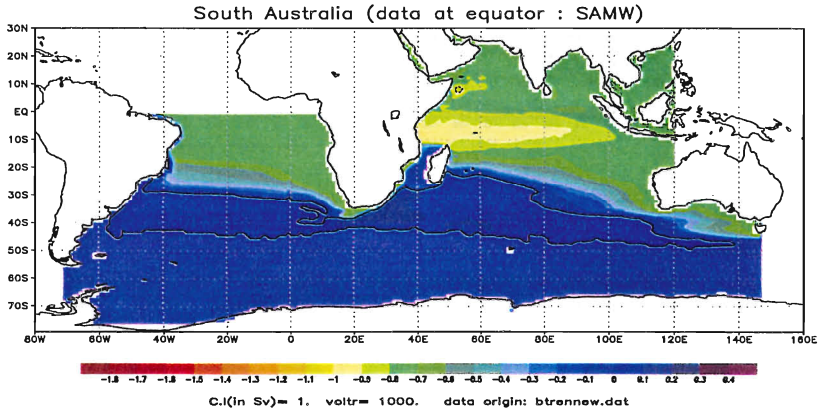

Figure 4.8: South Australia section btrend data file

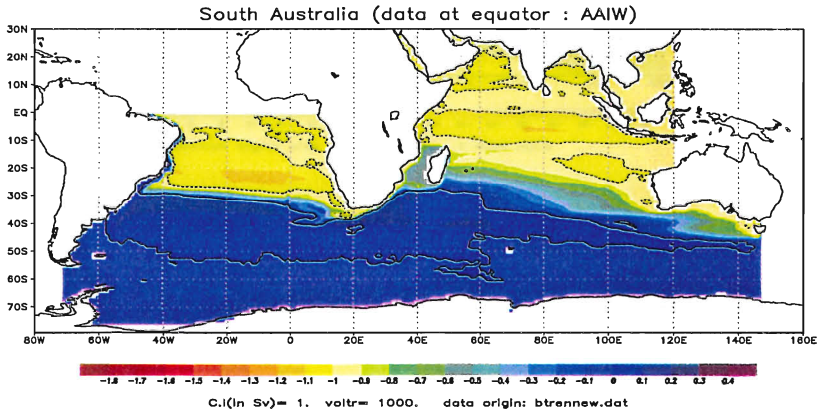

Figure 4.9: South Australia section btrend data file

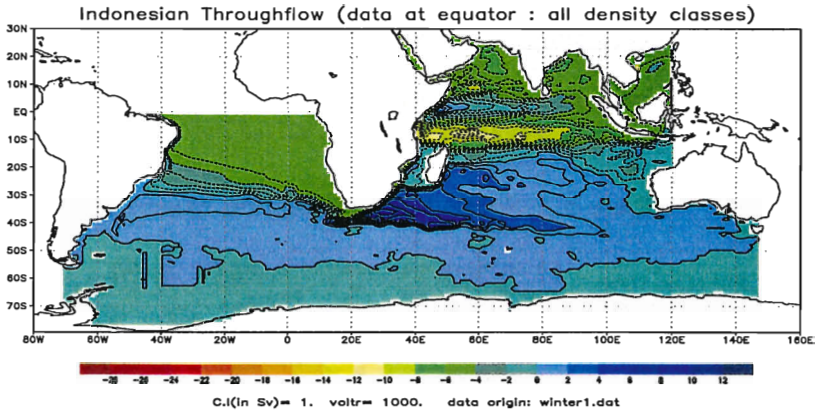

Figure 4.10: Indonesian Throughflow

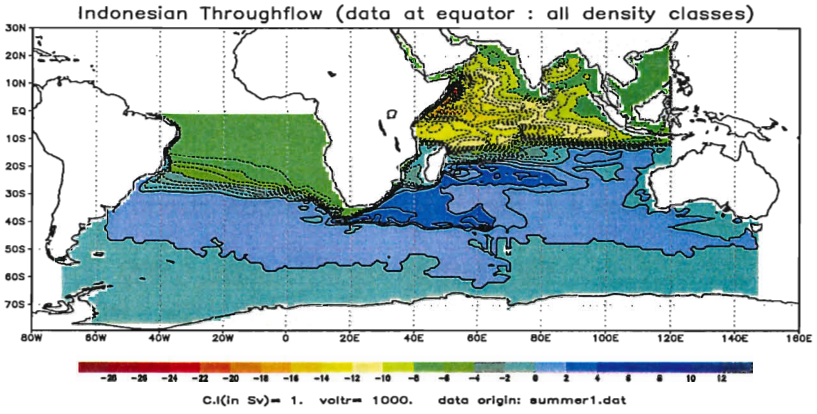

Figure 4.11: Indonesian Throughflow

4.2 The North Atlantic Deep Water

The North Atlantic Deep Water route has been calculated for water particles with both density above $\sigma_2 = 36.8$ and a southward flow, from the Atlantic Equator, tracing them forward to DRAKE, ITFL and SAUS. The recirculation is still the part of the water that reaches back the Atlantic Equator. A trajectory also represents 0,001 Sv (for same reasons). We also added three "virtual" sections at 60°S to check where the trajectories cross this latitude for the first time. These additional sections are :

1. Atlantic : from Drake to Africa ;
2. Indian West : from Africa to the middle of the Indian Ocean (IW), typically 80°E;
3. Indian East : from the middle of the Indian Ocean to south Australia (IE).

First of all, we noted that NADW mainly follows one route. The water particles reaching DRAKE or ITFL are insignificant (Tables 4.5, 4.6, 4.7), only 0,03 Sv (that means about 30 trajectories) when using the contribution of the exact bolus calculation + the contribution of the detrending. So we will only focus on the NADW route to the SAUS section that it represents 14,79 Sv on a total of 14,82 Sv when using the detrended data set.

The trajectories along this route cross the 60°S section between 20°E and 80°E (5,09 Sv) or flow directly to SAUS north to this latitude. Actually only 0,19 Sv cross this section between 80°E and SAUS, about 7,64 Sv reach SAUS north to 60°S. The transport through 60°S is nul between DRAKE and South of Africa (20°E).

The data sets used still have an importance when investigating NADW routes, both in term of transport and pathways of waters. Differences between the streamfunctions calculated from the annual mean velocity field or from the bolus velocity field are important for the vertical repartition of the water masses but less for the volume transport itself. With the annual data, most of the water (10,3 Sv) is LNADW ($37,0 < \sigma_2 \leq 37,1$), each of the other density class represents 1 v. With bolus data, 3,15 Sv are UNADW, 2,09 Sv are MNADW and only 7,99 Sv are LNADW compare to 10,3 Sv with the annual mean data set (Tables 4.5, 4.6).

On the other hand, differences between the results from the bolus data set and the detrended one are mainly related to the transport. The vertical structure of the streamfunctions is mostly the same. As long as the global structure of the streamfunctions is the same, the water mass volume transports through IW and SAUS are slightly different. Through IW, the transport is located in LNADW class. that is not the case through SAUS. It seems that the NADW upwells slowly flowing from 80°E to SAUS.

On global scale the NADW route has mostly the same structure when calculated from the three data sets : a strong southward boundary current along the South America until the flow reaches 45^{O}S. There it turns eastward, trapped by the Antarctic Circumpolar Current (ACC). On this way, some of the water recirculates around Cape Agulhas. The recirculation is more complicated when using both bolus and btrend velocity field than the annual mean data set. With the last one the recirculation is broader in the Indian Ocean. We also have a strong recirculation between 60^{O} and 70^{O} south and between 50^{O}W and 40^{O}E, then the water flows more or less straight to SAUS, there is only a southward deviation between 60^{O}E and 80^{O}S.

As we did for the upper branch of the Conveyor Belt, we calculated the streamfunctions from a seasonal data set. We also showed some big differences between seasons. Between summer and winter for instance, both the strength of water mass transport and the structure of this transport are different. Even if the boundary current seems to have the same structure, a lot of recirculations appear in the Atlantic Ocean with summer data. Using a summer data set, the strength of the boundary current seems to be weakened and there is much less activity around Cape Agulhas than using the winter velocity field. On the other hand, the circulation is broader in the Indian Ocean. With the summer data set, the recirculation in the Antarctic area is also weakened.

The volume transport below have been calculated at each section for Tables (4.5, 4.6, 4.7) for water coming from equator. Results are in Sverdrups (1 Sv = 10^6 m^3s^{-1}).

Table 4.5: Transport calculated from OCCAM annual mean.

Total	S	$D+I+S$	IW	IE	Recir
UNADW	0.95	0.96	0.01	0.01	2.49
MNADW	0.95	0.96	0.0	0.01	0.59
LNADW	10.29	10.30	4.45	1.01	19.98
REST	1.53	1.54	0.0	0.0	1.25
Total	13.72	13.77	4.46	1.03	24.31

Table 4.6: Transport calculated from annual mean + contribution from exact bolus calculation.

Total	S	$D+I+S$	IW	IE	Recir
UNADW	3.15	3.16	0.02	0.0	2.32
MNADW	2.09	2.09	0.02	0.0	1.81
LNADW	7.99	7.99	5.04	0.19	14.39
REST	0.62	0.65	0.0	0.0	1.42
Total	13.85	13.89	5.08	0.19	19.94

Table 4.7: Transport calculated from annual mean + contribution from exact bolus calculation + contribution from detrending.

Total	S	$D+I+S$	IW	IE	Recir
UNADW	3.49	3.50	0.02	0.0	2.33
MNADW	2.02	2.02	0.03	0.0	1.82
LNADW	8.09	8.09	5.04	0.05	14.39
REST	1.19	1.20	0.0	0.0	0.94
Total	14.79	14.82	5.09	0.05	19.48

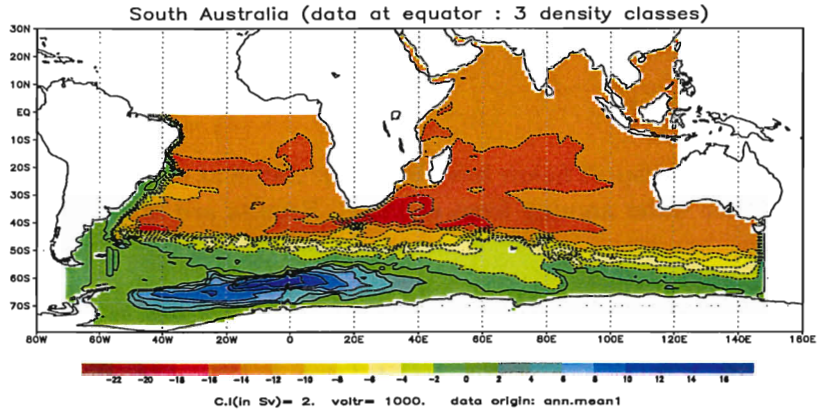

Figure 4.12: Drake section annual mean data file

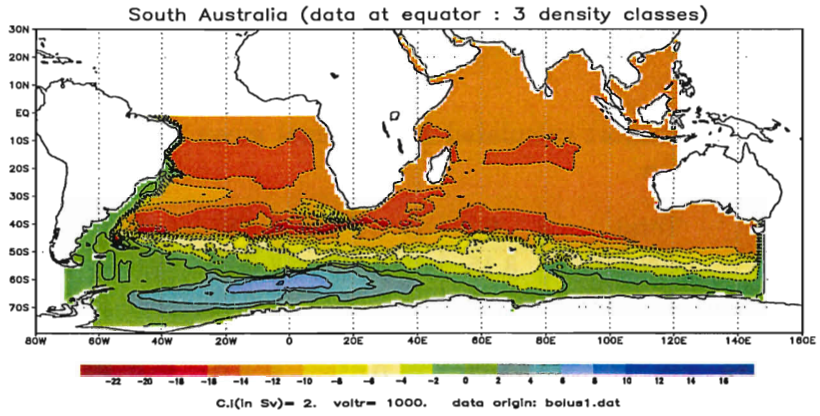

Figure 4.13: Drake section bolus data file

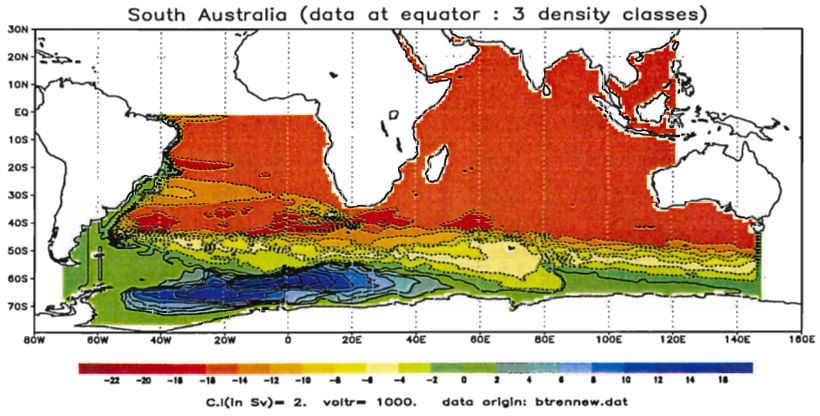

Figure 4.14: Drake section btrend data file

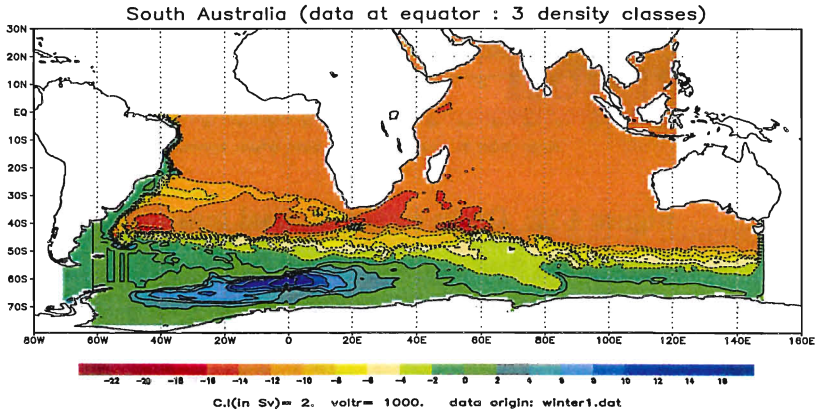

Figure 4.15: Drake section annual mean data file

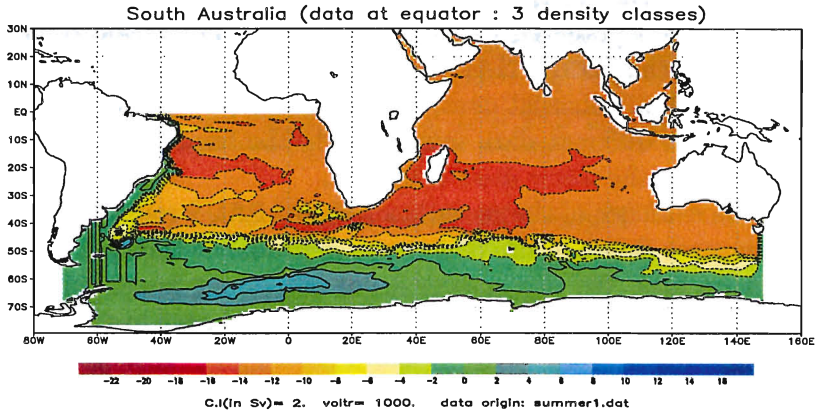

Figure 4.16: Drake section bolus data file

Chapter 5

Conclusion

We investigated in this study the resolution of the North Atlantic Deep Water and it upper layers return flow as parts of the Conveyor belt in the global ocean high resolution OCCAM model. We used in this way a Lagrangian methods which allow to trace a water masses as a set of trajectories calculated by a linear interpolation of the velocities inside a grid box thus through the entire ocean. This method is efficient as long as we use enough trajectories. We trajectories calculated from the equator to three sections : Drake Passage, Indonesian Throughflow and South Australia. Forward in time for the lower branch of the Conveyor Belt : the North Atlantic Deep Water defined as the water that flows southward with a potential density $\sigma_2 \geq 36.8$. And Backward in time for the upper branch, that is the NADW return flow defined as the water that flows northward with a potential density $\sigma_0 \leq 27.6$. The streamfunctions has been calculated from different data sets to study the impact of the bolus transport and the drift on the water mass transport.

We gave evidence of the recently suggested SAUS route in the upper branch of the Conveyor Belt but also of a season dependance transport both for NADW and it return flow. We also gave evidence of a strong impact of the bolus transport on both the routes and strength of the transport in OCCAM (that is an eddy-permitting model). The streamfunctions calculated from the detrended data set showed that the drift, induced by the not established steady state of the model, has also an impact but more on the strength of the transport than the water pathways.

We also have computed streamfunctions using a seasonal cycle, but this has been done too late to integrated results in this report.

These results and the results from the seasonal cycle will be used in an inter comparison study of the Conveyor Belt by the TRACMASS project team. In the future, it could be interesting to investigate further the impact of the seasonal cycle but also to the part of the transport that reaches the Bengulas Current or participate in the Agulhas retroflection as we suggested that this region is sensitive to both the season data set used and the bolus transport.

Bibliography

[1] Blanke B. and S. Raynaud. Kinematics of the pacific equatorial undercurrent : An eulerian and lagrangian approach from gcm results. *J. Phys. Oceanogr.*, 27:1038–1053, 1997.

[2] Broecker W.S. The great ocean conveyor. *Oceanography*, 4(2):79–89, 1991.

[3] Döös K. Interocean exchange of water masses. *J. Geophys. Res.*, 100:13499–13514, 1995.

[4] Drijfhout S.S., E. Maier-Reimer, and U. Mikolajewicz. Tracing the conveyor belt in the hamburg large-scale geostrophic ocean general circulation model. *J. Geophys. Res.*, 101:22563–22575, 1996.

[5] Georgi M. T. Modal propertie of antarctic intermerdiate water in the southeast pacific and the south atlantic. *J. Phys. Oceanogr.*, 9:456–468, 1979.

[6] Gordon A. L. Indian-atlantic transfer of thermocline water at the agulhas retroflection. *Science*, 227:1030–1033, 1985.

[7] Gordon A. L. Interocean exchange of thermocline water. *J. Geophys. Res.*, 91:5037–5046, 1986.

[8] Gordon A. L., R. F. Weiss, M. Smethie Jr., and M. J. Warner. Thermocline and intermediate water communication between the south atlantic and indian oceans. *J. Geophys. Res.*, 97:7223–7240, 1992.

[9] Killworth P. D. Deep convection in the world ocean. *Rev. Geophys.*, 21(1):1–26, 1983.

[10] Piola A. and D. Georgi. Circumpolar properties of antrctic intermediate water and subatntarctic mode water. *J. Phys. Oceanogr.*, 29:687–711, 1982.

[11] Rintoul S. R. South atlantic interbasin exchange. *J. Geophys. Res.*, 96:2675–2692, 1991.

[12] Schmitz W. J. On the interbasin-scale thermohaline circulation. *Rev. Geophys*, 33(2):151–173, 1995.

OVERZICHT VAN KNMI-PUBLICATIES, VERSCHENEN SEDERT 1999

KNMI-PUBLICATIE MET NUMMER

186-II Rainfall generator for the Rhine Basin: multi-site generation of weather variables by nearest-neighbour resampling / T. Brandsma a.o.
186-III Rainfall generator for the Rhine Basin: nearest-neighbour resampling of daily circulation indices and conditional generation of weather variables / Jules J. Beersma and T. Adri Buishand
186-IV Rainfall generator for the Rhine Basin: multi-site generation of weather variables for the entire drainage area / Rafal Wójcik, Jules J. Beersma and T. Adri Buishand
188 SODA workshop on chemical data assimilation: proceedings; 9-10 December 1998, KNMI, De Bilt, The Netherlands
189 Aardbevingen in Noord-Nederland in 1998: met overzichten over de periode 1986-1998 / [Afdeling SO]
190 Seismisch netwerk Noord-Nederland / [afdeling Seismologie]
191 Het KNMI-programma HISKLIM (HIStorisch KLIMaat) / Theo Brandsma, Frits Koek, Hendrik Wallbrink, Günther Können
192 Gang van zaken 1940-48 rond de 20.000 zoekgeraakte scheepsjournalen / Hendrik Wallbrink en Frits Koek

TECHNISCH RAPPORT = TECHNICAL REPORT (TR)

216 Evaluatierapport Automatisering Visuele Waarnemingen : Ontwikkeling Meestsystemen / Wiel Wauben en Hans de Jongh
217 Verificatie TAF en TREND / Hans van Bruggen
218 LEO - LSG and ECBILT coupled through OASIS: description and manual / A. Sterl
219 De invloed van de grondwaterstand, wind, temperatuur en dauwpunt op de vorming van stralingsmist: een kwantitatieve benadering / Jan Terpstra
220 Back-up modellering van windmeetmasten op luchthavens / Ilja Smits
221 PV-mixing around the tropopause in an extratropical cyclone / M. Sigmond
222 NPK-TIG oefendag 16 december 1998 / G.T. Geertsema, H. van Dorp e.a.
223 Golfhoogteverwachtingen voor de Zuidelijke Noordzee: een korte vergelijking van het ECMWF-golfmodel (EPS en operationeel), de nautische gidsverwachting, Nedwam en meteoroloog / D.H.P. Vogelezang, C.J. Kok
224 HDFg library and some HDF utilities: an extention to the NCSA HDF library user's manual & reference guide / Han The
225 The Deelen Infrasound Array: on the detection and identification of infrasound / L.G. Evers and H.W. Haak
226 2D Variational Ambiguity Removal / J.C.W. de Vries and A.C.M. Stoffelen
227 Seismo-akoestische analyse van de explosies bij S.E. Fireworks ; Enschede 13 mei 2000 / L.G. Evers en H.W. Haak
228 Evaluation of modified soil parameterization in the ECMWF landsurface scheme / R.J.M. IJpelaar
229 Evaluation of humidity and temperature measurements of Vaisala's HMP243 plus PT100 with two reference psychrometers / E.M.J. Meijer
230 [to be published later]
231 The Conveyor Belt in the OCCAM model: tracing water masses by a Lagrangian methodology / Trémeur Balbous and Sybren Drijfhout

WETENSCHAPPELIJK RAPPORT = SCIENTIFIC REPORT (WR)

99-01 Enhancement of solar and ultraviolet surface irradiance under partial cloudy conditions / Serdal Tunç
99-02 Turbulent air flow over sea waves: simplified model for applications / V.N. Kudryavtsev, V.K. Makin and J.F. Meirink
99-03 The KNMI Garderen experiment, micro-meteorological observations 1988-89: corrections / Fred C. Bosveld
99-04 ASGAMAGE: the ASGASEX MAGE experiment : final report / ed. W.A.Oost
00-01 A model of wind transformation over water-land surfaces / V.N. Kudryavtsev, V.K. Makin, A.M.G. Klein Tank and J.W. Verkaik
00-02 On the air-sea coupling in the WAM wave model / D.F.Doortmont and V.K. Makin.
00-03 Salmon's Hamiltonian approach to balanced flow applied to a one-layer isentropic model of the atmosphere / W.T.M. Verkley
00-04 On the behaviour of a few popular verification scores in yes-no forecasting / C.J. Kok
01-01 Hail detection using single-polarization radar / Iwan Holleman